O.A. YESHCHENKO, V.V. KOZACHENKO, A.V. TOMCHUK

Taras Shevchenko National University of Kyiv, Physics Department
(64/13, Volodymyrs'ka Str., Kyiv 01601, Ukraine; e-mail: yes@univ.kiev.ua)

SURFACE PLASMON RESONANCE IN "MONOLAYER OF Ni NANOPARTICLES/DIELECTRIC SPACER/Au (Ni) FILM" NANOSTRUCTURE: TUNING BY VARIATION OF SPACER THICKNESS [1]

UDC 539

The dual surface plasmon resonance in Ni nanoparticles in "monolayer of Ni nanoparticles/shellac film/Au (Ni) film" planar nanostructures has been observed in UV-vis absorption spectra. The dependences of the intensity, wavelength, and width of the dual SPR absorption peaks of Ni nanoparticles coupled with an Au (Ni) film on the spacer thickness have been studied in the range of spacer thicknesses of 12–43 nm. The main features of these dependences are an increase of the intensity, the blue shift, and the monotonic behavior of the widths of SPR absorption peaks at a decrease of the spacer thickness. The observed dependences have been rationalized as a result of the plasmonic coupling of the monolayer of Ni nanoparticles with the metal film and the variation of the dielectric permittivity of the environment of Ni nanoparticles caused by the metal film presence. The stronger dependences of the SPR spectral characteristics of Ni nanoparticles have been observed in the nanostructure containing the gold film comparing to that with a nickel one. Such effect is due to the stronger coupling of Ni nanoparticles with an Au film, and the stronger influence of an Au film on the permittivity of the environment of Ni nanoparticles.

K e y w o r d s: nickel nanoparticles, gold and nickel films, surface plasmons, plasmonic cavity, near-field coupling.

1. Introduction

The unique optical properties of metal nanoparticles (NPs) are well known, the source of which is due to the collective coherent excitations of free electrons in a nano-sized metal, also known as Surface Plasmon Resonance (SPR). Such properties are widely used in the applications of metal-based plasmonic nanostructures in biosensing, nanophotonics, and enhanced light emission [1–3]. Efficient and tunable absorption and scattering are essential for a variety of applications, such as designing the controlled-emissivity surfaces for thermophotovoltaic devices [4], tailoring an infrared spectrum for controlled thermal dissipation [5], producing detector elements for imaging [6], and AFM-IR nanospectroscopy [7]. Metamaterials based on metallic elements are particularly efficient at absorbing media, because both the electrical and the magnetic properties of a metamaterial can be tuned through a structured design [8]. Metamaterial absorbers and scatterers in the infrared and visible ranges have been fabricated, by using lithographically-patterned metallic structures [5, 9–13], rendering them inherently difficult to produce over large areas and hence reducing their applicability. The further enhancement of the performance of plasmonic devices requires new nanostructures with more easily tunable optical properties. Such structures are those with strong light-matter coupling, which leads to the hybridization of plasmonic modes therein. This goal is realized in metal NP – metal NP [14–18] and metal NP – metal film [19–31] configurations.

A particularly interesting plasmonic system under recent study is one consisting of a monolayer of metal NPs and a metal film, each separated by a dielectric film spacer of nanoscale thickness. This system has been predicted to display a wealth of interesting optical phenomena caused by the coupling of local-

[1] The paper was presented at the XXIII Galyna Puchkovska International School-Seminar "Spectroscopy of Molecules and Crystals".

ized surface plasmons of a nanoparticle with the delocalized thin film surface plasmon polariton, which is especially strong, when the nanoparticle is within a distance of approximately 50 nm from film's surface [19–31]. As has been reported in the literature, the absorption and scattering spectra of such systems are highly tunable with no effort to control the spatial arrangement of the metal NPs within their layer. The strong SPR-mediated coupling between the metal NPs and the metal film occurs in such a system. The coupling and the corresponding optical spectra of a metal NPs/film nanosystem can be tailored by varying the geometry (the size of NPs, the thickness of a spacer, and/or the thickness of a metal film). In this nanosystem, each metal NP is the optical analog of a grounded patch antenna, each with a nearly identical local field structure modified by the plasmonic response of metal's dielectric function, and each with an anomalously large absorption and scattering efficiency that can be partly attributed to the interferometric effect [30]. The absorptivity of a large surface area can easily be controlled in such system on scales out of reach of lithographic approaches (such as electron-beam lithography), which are otherwise required to manipulate the matter on the nanoscale.

In our present work, we studied the three-layer nanosystem arranged as described herein; the monolayer of nickel NPs was deposited on a glass substrate, and the Ni NPs' monolayer was covered by a nanoscale-thick dielectric shellac film. The nanoscale-thick metal film was then deposited on the external surface of a shellac film. We studied the samples with nickel and gold films covering the shellac one.

With respect to magneto-optical applications of metal-based nanostructures, magnetic metal NPs, Ni in particular, are attractive. Due to their interesting physical properties, nanostructures consisting of nickel and nickel oxide NPs have been widely studied, by using diverse methods [31–37]. The preparation and magnetic properties of nickel nanoparticles have been reported numerously, e.g. in Refs. [38–41]. However, the optical properties of Ni nanoparticles are studied rather poorly. We have found a few works reporting the results of optical studies of nickel nanoparticles in a sol-gel fabricated silica matrix [32, 37], in aqueous solutions [42], and fabricated by the Ni ion implantation in silica glass [43–45]. The most "famous" plasmonic nanoparticles are ones of noble metals: gold, silver, and copper. The nanoparticles of transition metals (Ni in particular) are characterized by a sufficiently slight manifestation of surface plasmons in optical spectra. That is due to the sufficiently higher damping of free electron oscillations in these metals. To our knowledge, our present work is the first one, where SPR in Ni NPs is studied not for isolated NPs, but for Ni NPs included in a near-field coupled plasmonic cavity of the type "monolayer of metal NPs/dielectric spacer/metal film". In our recent work [23], we studied the optical properties of a similar plasmonic cavity "monolayer of Au NPs/dielectric (shellac) spacer/Al film", where the strong plasmonic near-field coupling of gold NPs with an aluminum film was observed. We revealed the high ability of tuning absorption spectra of such nanostructure by the variation of the dielectric spacer thickness. Therefore, it is interesting to study the coupling effect in the plasmonic cavity containing NPs, where the SPR is considerably weaker than in noble metal NPs. Meanwhile, we studied the nanostructures containing a gold film with strong plasmonic optical response and a nickel film with weak plasmonic response to realize the stronger and weaker couplings of the monolayer of Ni NPs with a metal film in the plasmonic cavity.

Herein, we report the observation of two Ni NPs SPR peaks in the absorption spectra of the studied nanostructures and the influence of the dielectric shellac spacer thickness on the spectral characteristics (total intensity, spectral position, and width) of the Ni NPs SPR absorption peaks. The studies were performed in a spacer thickness interval of 12–43 nm. We revealed that the variation of the shellac spacer thickness influences the SPR in Ni NPs by two physical mechanisms: (1) the plasmonic near-field coupling of the Ni NPs with a metal film and (2) the variation of the dielectric permittivity of the Ni NPs environment. We obtained that stronger plasmonic coupling of Ni NPs with a metal film occurs in the sample containing the Au film than in the sample containing the Ni film.

2. Experimental. Sample Preparation and Characterization

The "Ni NPs monolayer/shellac film/Au film" and "Ni NPs monolayer/shellac film/Ni film" layered samples were prepared as follows. The optical glass plate with an area of 2.5×8 cm^2 was used. The nickel film was deposited by the thermal vacuum deposition on glass

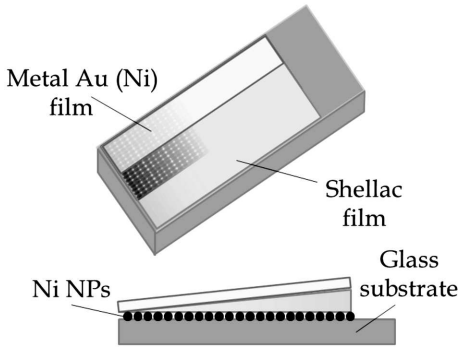

Fig. 1. Schematics for the studied "Ni NPs monolayer/shellac spacer/Au(Ni) film" nanostructure samples

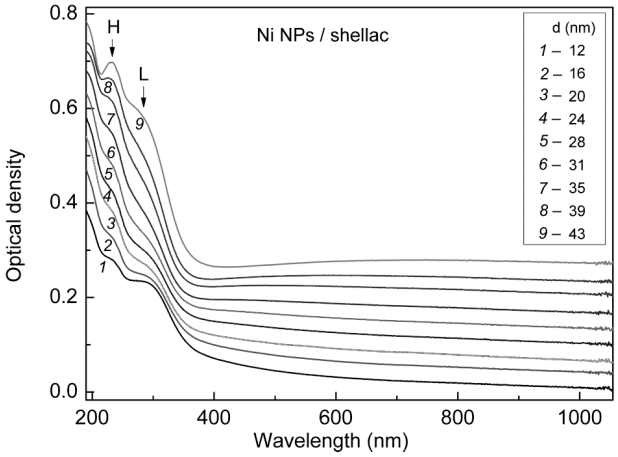

Fig. 2. Absorption spectra of the "Ni NPs monolayer/shellac film" nanostructure at various shellac film thicknesses in the interval of 12 nm $\leqslant l \leqslant$ 43 nm The spectra were shifted vertically for convenience. "H" and "L" mark the high and low energy SPR peaks of Ni NPs, respectively

as a strip 1.7 cm in width and 7 cm in length along the longer side of the plate, Fig. 1. The thickness of the deposited Ni film was about 10 nm. Then the sample with the Ni film was annealed at a temperature of 290 °C during 30 min. The annealing results in the transformation of the continuous nickel film to a monolayer of nickel NPs. The presence of Ni NPs on the glass substrate was confirmed by absorption spectra (Figs. 2–4).

After the annealing, the shellac film was deposited to the entire surface of the sample. The shellac film was deposited with monotonically variable thickness in the interval of 12–43 nm along the longer sample side, Fig. 1. At last, the thin metal (Au or Ni) film with thickness of 10 or 15 nm, respectively, was de-

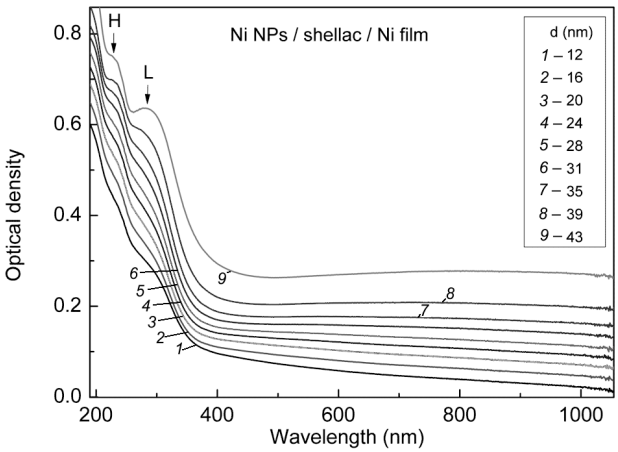

Fig. 3. Absorption spectra of the "Ni NPs monolayer/shellac film/Ni film" nanostructure at various shellac film thicknesses in the interval of 12 nm $\leqslant l \leqslant$ 43 nm. The spectra were shifted vertically for convenience. "H" and "L" mark the high and low energy SPR peaks of Ni NPs, respectively

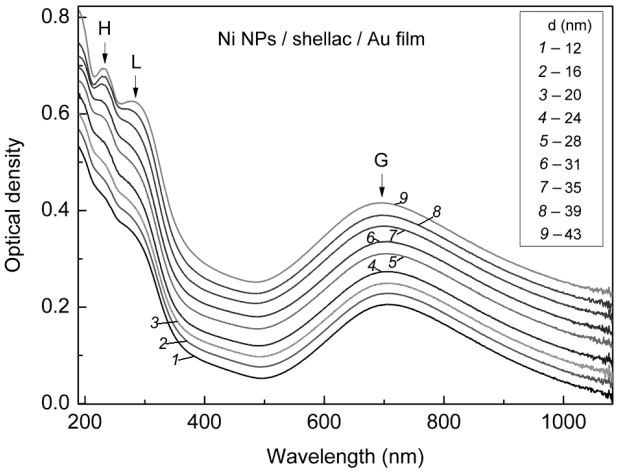

Fig. 4. Absorption spectra of the "Ni NPs monolayer/shellac film/Au film" nanostructure at various shellac film thicknesses in the interval of 12 nm $\leqslant l \leqslant$ 43 nm. The spectra were shifted vertically for convenience. "H" and "L" mark the high and low energy SPR peaks of Ni NPs, respectively, "G" marks the peak of SP polaritons in the Au film

posited on the sample area containing Ni NPs and the shellac film as a strip of 0.8 cm in width and 7 cm in length along the longer side of the plate, Fig. 1. Thus, the surface of the sample was divided into three zones. The first zone is a glass substrate covered by a shellac film, the second one is the Ni NPs monolayer on glass covered by a shellac film, and the third one is the Ni NPs monolayer on glass covered by

the shellac and metal (Au or Ni) films. The structure of the fabricated sample is shown in Fig. 1.

The films were deposited as follows. The metals (nickel and gold) and shellac were vacuum-evaporated from simple sources consisting of tungsten crucibles with shutters heated by an electric current. The crucibles were filled with a 99.99 purity metal and commercial grade purity shellac. The temperature in the crucible with a shellac powder was 250 °C, while the substrate was kept at 20 °C. During the shellac film deposition, the sample was installed at an angle to the molecular beam from the point evaporator to deposit the shellac film of variable thickness. The pressure in a vacuum chamber was about 10^{-5} Torr. The distance between substrates and filaments was about 15 cm. This large distance between substrates and filaments allowed us to produce quite uniform films. The thickness of films was controlled *in-situ* via deposition monitors, by using the quartz microbalance and *ex-situ* by multiangle incident ellipsometry.

The spectra of the optical density (absorption) of Ni NPs were measured. At the calculation of the optical density $D = \log(I_0/I)$: (1) for the sample area uncovered by a metal (Au or Ni) film, I_0 is the intensity of light passed through the glass and shellac film, and I is the intensity passed through the glass, Ni NPs layer, and shellac film; (2) for the sample area covered by a metal (Au or Ni) film, I_0 is the intensity of light passed through the glass, shellac and metal films, and I is the intensity passed through the glass, Ni NPs layer, shellac and metal films. Thus, the measured absorption spectra have no contribution of the absorption of a metal film. The UV–vis absorption spectra were measured using a Cary 60 UV-VIS spectrophotometer (Agilent Technologies, Inc.). The spectra were obtained at the normal incidence geometry, where the light beam was normal to the sample plane. The size of a light spot on the sample surface was 0.5×0.5 mm^2, so the shellac film thickness can be considered as constant within the area of a light spot. The absorption spectra were measured at room temperature.

3. Results and Discussion

We studied the UV–vis absorption spectra of the "Ni NPs/shellac film" (Fig. 2), "Ni NPs/shellac film/Ni film" (Fig. 3), and "Ni NPs/shellac film/Au film" (Fig. 4) nanostructures in the wide spectral range 190–1050 nm in dependence on the thickness of the dielectric shellac spacer in the interval of 12–43 nm. It is seen from the figures that two peaks with maxima in the interval 230–300 nm are in the spectra. We marked these peaks as H (high-energy) peak and L (low-energy) peak. Based on the data of Refs. [32, 37, 42–45], one can assume these peaks to originate from SPR in Ni NPs. However, why two peaks are observed? It is a common phenomenon, when the spherical metal particle has a single SPR. However, the NPs of metals with specific frequency-dependent dielectric permittivity $\varepsilon(\omega)$ with high contribution of the interband transitions into ε are characterized by two SPR modes, see, e.g., Ref. [46], where the observation of dual SPR in Zn NPs was reported. Due to the specific non-monotonic dependence $\varepsilon(\omega)$, the dipolar SPR condition

$$\min\left[(\varepsilon_1(\omega) + 2\varepsilon_m)^2 + \varepsilon_2^2(\omega)\right] \tag{1}$$

can be fulfilled at two different frequencies. Here, $\varepsilon_1(\omega)$ and $\varepsilon_2(\omega)$ are the real and imaginary parts of the metal dielectric permittivity, and ε_m is the permittivity of the host matrix. To check our above assumption of SPR nature of two observed peaks in absorption spectra of Ni NPs, we calculated the absorption spectra of isolated Ni NPs in dependence on the dielectric permittivity of the surrounding medium. According to the Mie theory of the light absorption by a spherical particle that is substantially smaller than the light wavelength, the absorption coefficient of the nanocomposite containing small isolated NPs is

$$\kappa(\omega) = \frac{9 f \varepsilon_m^{3/2} \omega}{c} \frac{\varepsilon_2(\omega)}{\left(\varepsilon_1(\omega) + 2\varepsilon_m\right)^2 + \varepsilon_2^2(\omega)}, \tag{2}$$

where f is the filling factor of the nanocomposite, and c is the light velocity. In the calculations, we took the frequency dependence of the nickel permittivity from Ref. [47]. The calculation results are presented in Fig. 5. One can see that, similarly to experimental absorption spectra, the calculated ones contain two SPR peaks. It is seen from Fig. 5 that the wavelengths of both H and L peaks depend on the permittivity of the surrounding medium, i.e. the peaks are red-shifted at the increase of ε_m, which is the well-known phenomena for SPR in metal NPs. Since the permittivity of the surrounding medium influences only the surface electronic excitations of the NP and does not influence the bulk excitations, the dependence of the wavelengths of H and L peaks on ε_m

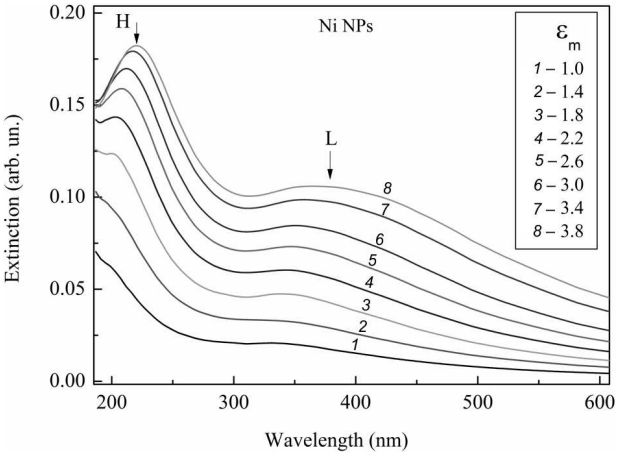

Fig. 5. Calculated absorption spectra of Ni NPs in dependence on the dielectric permittivity of the host matrix. The spectra were shifted vertically for convenience. "H" and "L" mark the high- and low-energy SPR peaks of Ni NPs, respectively

allows us to attribute both H and L peaks to SPR in Ni NPs. The similar behavior of the wavelengths of absorption peaks for Ni NPs is observed experimentally. The wavelengths of both peaks are red-shifted with increasing the shellac thickness. Indeed, an increase of the shellac film thickness would cause an increase of the permittivity of the Ni NPs environment that would lead to the red shift of SPR. Thus, Figs. 2–4 prove the presence of Ni NPs in the studied nanostructures and the existence of the dual dipolar SPR in Ni NPs.

Let us analyze the behavior of the experimental absorption spectra of the nanostructures containing the metal Au (Ni) film and without it, Figs. 2–4. It is apparent that the spectra depend on the shellac film thickness for all the samples. To quantitatively analyze the effects of the spacer thickness on SPR peaks' spectral characteristics (intensity – total area, wavelength, and width), the spectra were fitted with basic Gaussian peaks. The dependences of SPR spectral characteristics on the spacer thickness are caused both by a change of the influence of a metal film and a change of the surrounding medium permittivity occurring at the variation of the shellac spacer thickness. To extract the contribution of the metal film on SPR in Ni NPs, we took the sample area "Ni NPs/shellac film" without a metal film as a reference, i.e. we calculated: (1) the ratio of the intensities of SPR peaks for the sample area containing a metal film and for the area without metal film $I_{\mathrm{Ni/shellac/metal}}(l)/I_{\mathrm{Ni/shellac}}(l)$; (2) the SPR spectral shift $\lambda_{\mathrm{Ni/shellac/metal}}(l) - \lambda_{\mathrm{Ni/shellac}}(l)$; (3) the ratio of the SPR peak widths $\Delta\lambda_{\mathrm{Ni/shellac/metal}}(l)/\Delta\lambda_{\mathrm{Ni/shellac}}(l)$. As zero points for the dependences, we took the respective values at the maximal shellac thickness $l = 43$ nm. The respective experimental dependences are shown in Figs. 6, *a–c*. Based on the calculated absorption spectra of Ni NPs, we also obtained the dependences of the spectral characteristics of SPR absorption peaks on the surrounding medium permittivity, Figs. 7, *a–c*.

The main features of the dependences of the Ni NPs SPR spectral characteristics on the spacer thickness are as follows. The first feature is an increase of the SPR absorption peak intensity at a decrease of the spacer thickness that is observed for both "Ni NPs/shellac film/Ni film" and "Ni NPs/shellac film/Au film" nanostructures, Fig. 6, *a*. We note that an increase of the light absorption with decreasing the spacer thickness is stronger for the sample with a gold film. Indeed, upon decreasing the spacer thickness from 43 nm to 12 nm, the intensity of H peak increases by 3.4 times for the sample with the Au film and by 2.2 times for the sample with the Ni film, the intensity of L peak increases by 2.0 times for the sample with the Au film and by 1.4 times for the sample with the Ni film, see Fig. 6, *a*. Thus, we can conclude that there is an appreciable enhancement of the light absorption by Ni NPs in the presence of a metal film; this is in agreement with the literature [20, 21, 23, 31]. Let us discuss the physical mechanisms of the observed effect of varying the dielectric spacer thickness on the light absorption intensity. The first possible mechanism can be a change of the dielectric permittivity of the Ni NPs environment. Indeed, since the real part of the permittivity of a metal film is negative, the approaching of a metal film to Ni NPs with decreasing the shellac film thickness would lead to a decrease in the surrounding medium permittivity, that, in accordance with Fig. 7, *a*, would lead to a decrease of the SPR peak intensity. However, we observed experimentally the opposite dependence, Fig. 6, *a*. The second possible cause for the observed dependence of the intensity of SPR peaks on the shellac film thickness can be the following. The light scattered by Ni NPs consists of electromagnetic waves with a large curvature of the wave-front, which can excite the surface plasmon po-

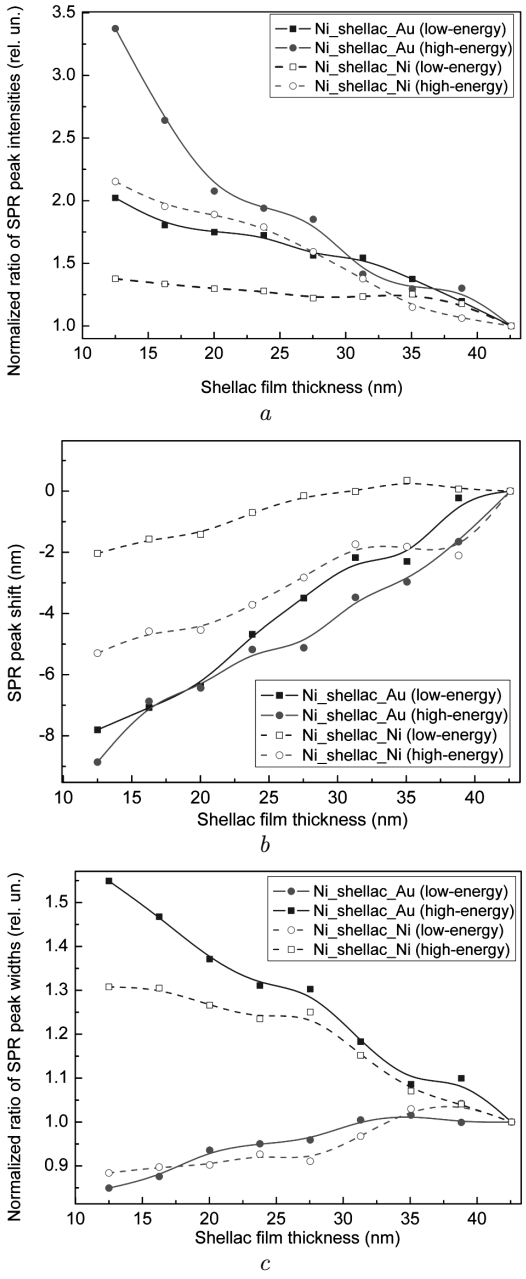

Fig. 6. Behavior of the spectral characteristics of SPR absorption peaks of Ni NPs in the "Ni NPs monolayer/shellac film/Au(Ni) film" nanostructure with variation of the shellac film thickness: the dependence of the normalized ratio of the SPR peak intensities (*a*), SPR peak spectral shift (*b*), and normalized ratio of the SPR peak widths for Ni NPs in the "Ni NPs monolayer/shellac film/Au(Ni) film" nanostructure in relation to Ni NPs in the "Ni NPs monolayer/shellac film" one. The lines are added to guide an eye, when analyzing the character of dependences

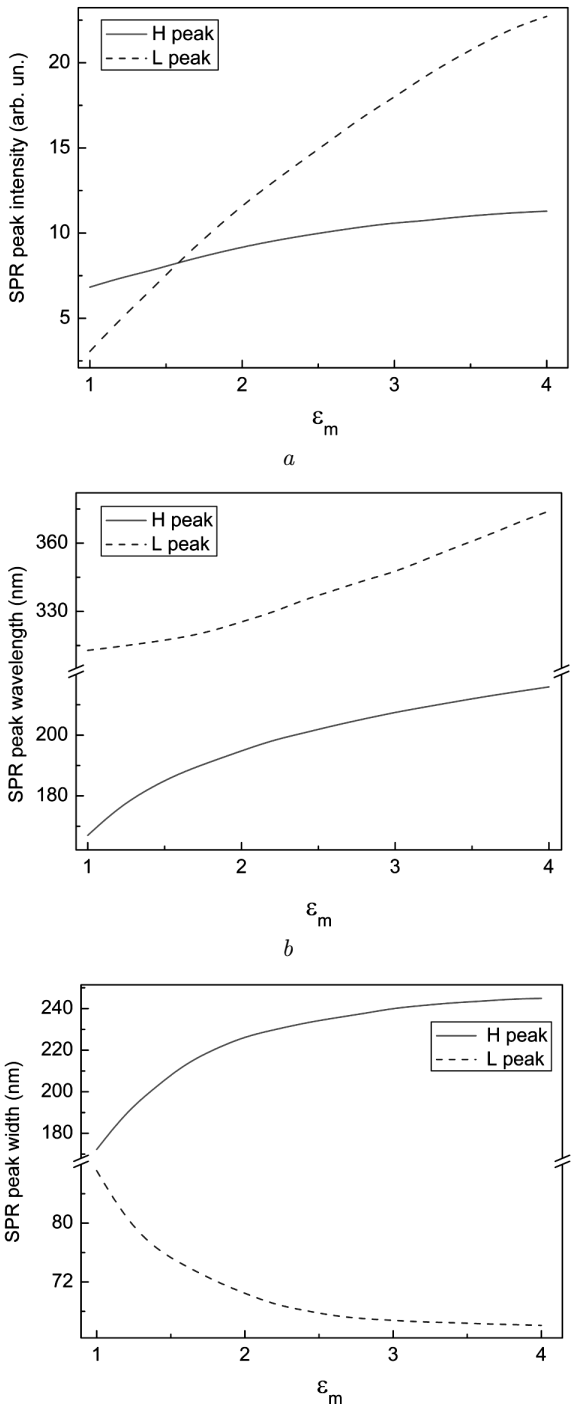

Fig. 7. Calculated dependences of the spectral characteristics of SPR absorption peaks of Ni NPs on the dielectric permittivity of the host matrix: peak intensities (*a*), peak wavelength (*b*), and peak widths (*c*)

laritons (SPPs) in the metal film, i.e. propagating SP modes. Therefore, aside from the light absorption by Ni NPs themselves, the additional energy dissipation of the incident light beam occurs due to the SPP excitation in a metal film, resulting in an additional light absorption. With a decrease in the spacer thickness, the Ni NPs are approaching the metal (Au, Ni) film, and, correspondingly, the excitation of SPPs occurs more efficiently. The more efficient SPP excitation leads to the increased dissipation of the incident light energy and, correspondingly, to an increase in the absorption intensity. The fact of a stronger increase of the absorption in the sample containing the gold film comparing to one containing the nickel film is due to the stronger plasmonic coupling of the monolayer of Ni NPs with the Au film than with the Ni film. It is due to the fact that the damping of plasma oscillations in gold is considerably weaker than in nickel. Thus, the excitation of SPPs in the Au film occurs more efficiently than in the Ni film. An additional evidence of the excitation of SPPs in the gold film is the existence of a broad G peak in the absorption spectra of the "Ni NPs/shellac film/Au film" sample with maximum at about 700 nm (Fig. 4). The SPPs in the Au film can be excited only by near-field waves of light scattered by Ni NPs, since the direct excitation of SPPs in a flat metal film by a flat wave of the external light beam is forbidden by the momentum conservation law. We note that the additional peak caused by the excitation of SPPs in a metal film is absent in the spectra of the sample containing the Ni film. It is due to the sufficiently less efficient excitation of SPPs in the Ni film than in the Au film, which is a result of the sufficiently stronger damping of plasma oscillations in nickel than in gold. Another source of the increased plasmonic absorption peak intensity may be due to the fact that light scattered by Ni NPs is reflected from the metal film back to the Ni NPs layer and is then reabsorbed.

A second feature is a monotonous blue shift of both H and L peaks at a decrease of the spacer thickness, Fig. 6, *b*. We note that, like the dependences of the SPR peaks intensities on the spacer thickness (Fig. 6, *a*), the dependences of the wavelengths of SPR peaks on the spacer thickness are stronger for Ni NPs in the sample with the Au film than for Ni NPs in the sample with the Ni film. Let us discuss the physical mechanisms of the observed effect of the varying dielectric spacer thickness on the wavelength of SPR peaks. The first possible mechanism can be a change of the strength of the plasmonic coupling of Ni NPs with a metal film. Indeed, a decrease of the spacer thickness leads to approaching Ni NPs to the metal film that would cause the strengthening of the coupling. As was reported in recent works [19, 21–23], the strengthening of the coupling leads to a red shift of the SPR peak of metal nanoparticles coupled with a metal film. However, we observed the red shift of SPR peaks with decreasing the spacer thickness. Therefore, one can conclude that the coupling of Ni NPs with an Au (Ni) film is not the dominant mechanism of the spectral shift of SPR peaks of Ni NPs in the samples with metal films. The second possible mechanism of the observed SPR shift can be a change of the permittivity of the Ni NPs environment. Indeed, since the real part of the permittivity of a metal film is negative, the approaching of the metal film to Ni NPs with decreasing the shellac film thickness would lead to a decrease of the surrounding medium permittivity ε_m. According to the result of calculations of the dependence of the wavelengths of SPR peaks in Ni NPs on the surrounding medium permittivity (Fig. 7, *b*), such decrease of ε_m would lead to a blue shift of the SPR peaks that is observed experimentally, Fig. 6, *b*. Thus, one can conclude that the observed blue shift of SPR H and L peaks of Ni NPs with decreasing the spacer thickness originates from a decrease of the permittivity of surrounding medium caused by approaching the metal film to the Ni NPs monolayer. The stronger blue shift of SPR peaks of Ni NPs in the sample with a gold film compared to that in the sample with a nickel film is due to a smaller value of the real part of the permittivity of gold than that of nickel at SPR wavelengths, e.g., at $\lambda = 300$ nm: $\varepsilon_1^{(\mathrm{Au})} = -1.23$ and $\varepsilon_1^{(\mathrm{Ni})} = -0.67$. Therefore, a decrease of ε_m caused by a metal film is stronger in the sample with the Au film than in the sample with the Ni film.

A third feature is the monotonous change of the widths of H and L SPR peaks of Ni NPs with the variation of the spacer thickness, Fig. 6, *c*. One can see that H peak broadens at a decrease of the spacer thickness, while L peak narrows. Such dependences are similar for Ni NPs in the sample with the Au film and with the Ni film. We note that, like the dependences of the intensities of SPR peaks and wavelengths on the spacer thickness (Fig. 6, *a, b*), the de-

pendences of the widths of SPR peaks on the spacer thickness are stronger for Ni NPs in the sample with the Au film than for Ni NPs in the sample with the Ni film. It is seen that the behavior of the widths of H and L peaks at a decrease of the spacer thickness (Fig. 6, *c*) is similar to the calculated behavior of the widths of H and L peaks at a decrease of the permittivity of the surrounding medium ε_m. In view of the above considerations of a decrease of ε_m with decreasing the spacer thickness, we can conclude that the observed change of the widths of H and L peaks with decreasing the spacer thickness is due to a decrease of ε_m caused by approaching the metal film to the monolayer of Ni NPs. Like the dependences of the intensities of SPR peaks and wavelengths, the stronger dependences of the widths of SPR peaks for Ni NPs observed in the sample with the gold film than that in the sample with the nickel film are a result of the stronger decrease of ε_m with decreasing the spacer thickness in the sample with the Au film due to the smaller real part of the permittivity of gold comparing to that of nickel at the SPR wavelengths.

4. Conclusions

The dual SPR in Ni NPs in "monolayer of Ni nanoparticles/shellac film/Au (Ni) film" planar nanostructures is observed. The dependences of the spectral characteristics (intensity, wavelength and width) of the SPR absorption peaks of Ni NPs coupled with an Au (Ni) film on the spacer thickness are studied in the interval of thicknesses of 12–43 nm. The main features of these dependences are an increase of the intensities, the blue shift, and the monotonic behavior of the widths of SPR absorption peaks at a decrease of the spacer thickness. The noticeable enhancement (by 3.4 times in the sample containing the Au film, and by 2.1 times in the sample with the Ni film) of light absorption by the Ni NPs monolayer in the presence of a metal film is observed, as compared to the same monolayer without a metal film. The increase of the light absorption in the samples containing a metal film was rationalized as a result of the plasmonic coupling of the monolayer of Ni NPs with a metal film that causes the excitation of surface plasmon polaritons in a metal film. Meanwhile, the spectral shift and a change of the widths of SPR peaks are explained as a result of the decrease of the dielectric permittivity of the Ni NPs environment occurring at approaching the metal film to the Ni NPs monolayer at a decrease of the spacer thickness. The stronger dependences of the SPR spectral characteristics of Ni NPs on the spacer thickness are observed in the sample containing the gold film than in the sample with the Ni film. It is due to the stronger coupling of Ni NPs with the Au film, as well as to the stronger influence of the Au film on the permittivity of the Ni NPs environment comparing to the Ni film.

This work was supported by the NATO Science for Peace and Security (SPS) Program (grant NUKR.SFPP 984617).

1. E. Ozbay. Plasmonics: merging photonics and electronics at nanoscale dimensions. *Science* **311**, 189 (2006).
2. W.L. Barnes, A. Dereux, T.W. Ebbesen. Surface plasmon subwavelength optics. *Nature* **424**, 824 (2003).
3. M. I. Stockman. Nanoplasmonics: past, present, and glimpse into future. *Opt. Express* **19**, 22029 (2011).
4. P. Bermel, M. Ghebrebrhan, W. Chan, Y.X. Yeng, M. Araghchini, R. Hamam, C.H. Marton, K.F. Jensen, M. Soljacič, J.D. Joannopoulos, S.G. Johnson, I. Celanovic. Design and global optimization of high-efficiency thermophotovoltaic systems. *Opt. Express* **18**, A314 (2010).
5. J. Hao, J. Wang, X. Liu, W.J. Padilla, L. Zhou, M. Qiu. High performance optical absorber based on a plasmonic metamaterial. *Appl. Phys. Lett.* **96**, 251104 (2010).
6. F. Niesler, J. Gansel, S. Fischbach, M. Wegener. Metamaterial metal-based bolometers. *Appl. Phys. Lett.* **100**, 203508 (2012).
7. L. Baldassarre, V. Giliberti, A. Rosa, M. Ortolani, A. Bonamore, P. Baiocco, K. Kjoller, P. Calvani, A. Nucara. Mapping the amide I absorption in single bacteria and mammalian cells with resonant infrared nanospectroscopy. *Nanotechnology* **27**, 075101 (2016).
8. N.I. Landy, S. Sajuyigbe, J.J. Mock, D.R. Smith, W.J. Padilla. Perfect metamaterial absorber. *Phys. Rev. Lett.* **100**, 207402 (2008).
9. Y. Avitzour, Y.A. Urzhumov, G. Shvets. Wide-angle infrared absorber based on a negative-index plasmonic metamaterial. *Phys. Rev. B* **79**, 045131 (2009).
10. N. Liu, M. Mesch, T. Weiss, M. Hentschel, H. Giessen. Infrared perfect absorber and its application as plasmonic sensor. *Nano Lett.* **10**, 2342 (2010).
11. C. Koechlin, P. Bouchon, F. Pardo, J. Jaeck, X. Lafosse, J.-L. Pelouard, R. Haïdar. Total routing and absorption of photons in dual color plasmonic antennas. *Appl. Phys. Lett.* **99**, 241104 (2011).
12. C. Wu, B. Neuner, G. Shvets, J. John, A. Milder, B. Zollars, S. Savoy. Large-area wide-angle spectrally selective plasmonic absorber. *Phys. Rev. B* **84**, 075102 (2011).
13. A. Tittl, P. Mai, R. Taubert, D. Dregely, N.L.H. Giessen. Palladium-based plasmonic perfect absorber in the visible wavelength range and its application to hydrogen sensing. *Nano Lett.* **11**, 4366 (2011).

14. E. Prodan, C. Radloff, N. J. Halas, P. Nordlander. A hybridization model for the plasmon response of complex nanostructures. *Science* **302**, 419 (2003).
15. O.A. Yeshchenko, I. Bondarchuk, S. Malynych, Yu. Galabura, G. Chumanov, I. Luzinov. Surface plasmon modes of sandwich-like metal–dielectric nanostructures. *Plasmonics* **10**, 655 (2015).
16. V.V. Kravets, O.A. Yeshchenko, V.V. Gozhenko, L.E. Ocola, D.A. Smith, J.V. Vedral, A.O. Pinchuk. Electrodynamic coupling in regular arrays of gold nanocylinders. *J. Phys. D* **45**, 045102 (2012).
17. M. Hentschel, M. Saliba, R. Vogelgesang, H. Giessen, A.P. Alivisatos, N. Liu. Transition from isolated to collective modes in plasmonic oligomers. *Nano Lett.* **10**, 2721 (2010).
18. M. Ringler, A. Schwemer, M. Wunderlich, A. Nichtl, K. Kürzinger, T.A. Klar, J. Feldmann. Shaping emission spectra of fluorescent molecules with single plasmonic nanoresonators. *Phys. Rev. Lett.* **100**, 203002 (2008).
19. A. Moreau, C. Ciracì, J.J. Mock, R.T. Hill, Q. Wang, B.J. Wiley, A. Chilkoti, D.R. Smith. Controlled-reflectance surfaces with film-coupled colloidal nanoantennas. *Nature* **492**, 86 (2012).
20. J.J. Mock, R.T. Hill, A. Degiron, S. Zauscher, A. Chilkoti, D.R. Smith. Distance-dependent plasmon resonant coupling between a gold nanoparticle and gold film. *Nano Lett.* **8**, 2245 (2008).
21. C. Ciracì, R.T. Hill, J.J. Mock, Y. Urzhumov, A.I. Fernández-Domínguez, S.A. Maier, J.B. Pendry, A. Chilkoti, D.R. Smith. Probing the ultimate limits of plasmonic enhancement. *Science* **337**, 1072 (2012).
22. A. Sobhani, A. Manjavacas, Y. Cao, M.J. McClain, F.J. García de Abajo, P. Nordlander, N. J. Halas. Pronounced linewidth narrowing of an aluminum nanoparticle plasmon resonance by interaction with an aluminum metallic film. *Nano Lett.* **15**, 6946 (2015).
23. O.A. Yeshchenko, V.V. Kozachenko, Yu.F. Liakhov, A.V. Tomchuk, M. Haftel, A.O. Pinchuk. Gold nanoparticle plasmon resonance in near-field coupled Au NPs layer/Al film nanostructure: dependence on metal film thickness. *Mater. Res. Express* **4**, 106401 (2017).
24. A. Pinchuk, A. Hilger, G. von Plessen, U. Kreibig. Substrate effect on the optical response of silver nanoparticles. *Nanotechnology* **15** 1890 (2004).
25. N. Papanikolaou. Optical properties of metallic nanoparticle arrays on a thin metallic film. *Phys. Rev. B* **75**, 235426 (2007).
26. P. Nordlander, F. Le. Plasmonic structure and electromagnetic field enhancements in the metallic nanoparticle-film system. *Appl. Phys. B* **84**, 35 (2006).
27. F. Le, N.Z. Lwin, J.M. Steele, M. Kall, N.J. Halas, P. Nordlander. Plasmons in the metallic nanoparticle-film system as a tunable impurity problem. *Nano Lett.* **5**, 2009 (2005).
28. N. Nedyalkov, T. Sakai, T. Miyanishi, M. Obara. Near field distribution in two dimensionally arrayed gold nanoparticles on platinum substrate. *Appl. Phys. Lett.* **90**, 123106 (2007).
29. G. Leveque, O.J.F. Martin. Optical interactions in a plasmonic particle coupled to a metallic film. *Opt. Express* **14**, 9971 (2006).
30. S.K. Eah, H.M. Jaeger, N.F. Scherer, G.P. Wiederrecht, X.M. Lin. Scattered light interference from a single metal nanoparticle and its mirror image. *J. Phys. Chem. B* **109**, 11858 (2005).
31. W. Wan, Y. Chong, L. Ge, H. Noh, A. D. Stone, H. Cao. Time-reversed lasing and interferometric control of absorption. *Science* **331**, 889 (2011).
32. O.A. Yeshchenko, I.M. Dmitruk, A.A. Alexeenko, A.M. Dmytruk. Optical properties of sol–gel fabricated Ni/SiO_2 glass nanocomposites. *J. Phys. Chem. Solids* **69**, 1615 (2008).
33. S. Roy, D. Das, C. Chakravorty, D.C. Agrawal. Magnetic properties of glass–metal nanocomposites prepared by the sol–gel route and hot pressing. *J. Appl. Phys.* **74**, 4746 (1993).
34. L. Nárvaez, O. Domínguez, J.R. Martínez, F. Ruiz. Preparation of $(Ni-B)/SiO_2$, Ni/SiO_2 and NiO/SiO_2 nanocomposites. *J. Non-Cryst. Solids* **318**, 37 (2003).
35. M.A. Ermakova, D.Yu. Ermakov, S.V. Cherepanova, L.M. Plyasova. Synthesis of ultradispersed nickel particles by reduction of high-loaded $NiO–SiO_2$ systems prepared by heterophase sol-gel method. *J. Phys. Chem. B* **106**, 11922 (2002).
36. K. Takeuchi, T. Isobe, M. Senna. Effects of mechanical pretreatment of precursor sols and gels on the formation of NiO/SiO_2 composites with a controlled microstructure. *J. Non-Cryst. Solids* **194**, 58 (1996).
37. J. Hernández-Torres, A. Mendoza-Galván. Optical properties of sol-gel SiO_2films containing Nickel. *Thin Solid Films* **472**, 130 (2005).
38. N. Cordente, M. Respaud, F. Senocq, M.-J. Casanove, C. Amiens, B. Chaudret. Synthesis and Magnetic Properties of Nickel Nanorods. *Nano Lett.* **1**, 565 (2001).
39. C. Estournes, T. Lutz, T. Happich, T. Quaranta, P. Wissler, J.L. Guille. Nickel nanoparticles in silica gel: Preparation and magnetic properties. *J. Magn. Magn. Mater.* **173**, 83 (1997).
40. J. Jiao, S. Seraphin, X. Wang, J.C. Withers. Preparation and properties of ferromagnetic carboncoated Fe, Co, and Ni nanoparticles. *J. Appl. Phys.* **80**, 103 (1996).
41. F.C. Fonseca, G.F. Goya, R.F. Jardim, R. Muccillo, N.L.V. Carreño, E. Longo, E.R. Leite. Superparamagnetism and magnetic properties of Ni nanoparticles embedded in SiO_2. *Phys. Rev. B* **66**, 104406 (2002).
42. B.G. Ershov. Aqueous solutions of colloidal nickel: Radiation-chemical preparation, absorption spectra, and properties. *Russian Chemical Bulletin* **49**, 1715 (2000).
43. H. Amekura, Y. Takeda, H. Kitazawa, N. Kishimoto. Modification of metal nanoparticles in SiO_2 by thermal oxidation. *SPIE Proc.* **4977**, 639 (2003).
44. T. Isobe, S.Y. Park, R.A. Weeks, R.A. Zhur. The optical and magnetic properties of Ni^+-implanted silica. *J. Non-Cryst. Solids* **189**, 173 (1995).

45. O. Cíntora-González, C. Estournès, D. Muller, J. Guille, J.J. Grob. Magnetic behavior of Ni^+ implanted silica. *Nucl. Instr. Meth. B* **147**, 422 (1999).
46. H. Amekura, N. Umeda, K. Kono, Y. Takeda, N. Kishimoto, Ch. Buchal, S. Mantl. Dual surface plasmon resonances in Zn nanoparticles in SiO_2: An experimental study based on optical absorption and thermal stability. *Nanotechnology* **18**, 395707 (2007).
47. P.B. Johnson, R.W. Christy. Optical constants of transition metals: Ti, V, Cr, Mn, Fe, Co, Ni, and Pd. *Phys. Rev. B* **9**, 5056 (1974).

Received 22.02.18

О.А. Єщенко, В.В. Козаченко, А.В. Томчук

ПОВЕРХНЕВИЙ ПЛАЗМОННИЙ РЕЗОНАНС У НАНОСТРУКТУРІ “МОНОШАР НАНОЧАСТИНОК Ni/ДІЕЛЕКТРИЧНИЙ ПРОШАРОК/ПЛІВКА Au (Ni)”: ЗМІНА ШЛЯХОМ ВАРІАЦІЇ ТОВЩИНИ ДІЕЛЕКТРИЧНОГО ПРОШАРКУ

Р е з ю м е

Подвійний поверхневий плазмонний резонанс спостерігався у спектрах поглинання наночастинок Ni у планарних наноструктурах “моношар наночастинок Ni/плівка шелаку/плівка Au (Ni)”. Залежності інтенсивності, довжини хвилі та півширини плазмонних піків поглинання наночастинок Ni, взаємодіючих з плівкою Au (Ni), від товщини діелектричного прошарку було досліджено в діапазоні товщин прошарку 12–43 нм. Основними особливостями цих залежностей є збільшення інтенсивності, блакитний зсув та монотонна поведінка півширини плазмонних піків поглинання при зменшенні товщини діелектричного прошарку. Спостережувані залежності були інтерпретовані як результат плазмонної взаємодії моношару наночастинок Ni з металевою плівкою та зміни діелектричної проникності середовища, оточуючого наночастинки Ni, що спричинена присутністю плівки металу. Для наноструктури, що містить плівку золота, спостерігалися сильніші залежності спектральних характеристик поверхневого плазмонного резонансу наночастинок Ni, ніж для наноструктури з плівкою нікелю. Цей ефект зумовлений сильнішою взаємодією наночастинок Ni з плівкою Au та сильнішим впливом плівки Au на діелектричну проникність середовища, оточуючого наночастинки Ni.